processes

MDPI

Article

A Novel Security Framework for the Enhancement of the Voltage Stability in a High-Voltage Direct Current System

Ibrahim Alsaduni

Department of Electrical Engineering, College of Engineering, Majmaah University, Al-Majmaah 11952, Saudi Arabia; i.alsaduni@mu.edu.sa

Abstract: Due to financial limitations, power systems are being operated closer to their stability boundaries. Voltage stability analysis is crucial to preserve a power system's equilibrium. However, this impacts a system's dependability and security, and maintaining a power system's voltage stability is a difficult challenge. Additionally, the inverters and converters in a high-voltage direct current (HVDC) system use a significant amount of reactive power, which exacerbates voltage instability. In this study, a new algorithm called Adaptive Neural Spider Monkey (ANSMA) was developed to improve the voltage stability security in an HVDC system. Additionally, the proposed ANSMA maintains voltage stability while scheduling the loads in the generator. Moreover, applying artificial-intelligence-related energy systems to these issues is considered an efficient solution. Fuzzy, neural, ANN, and other improvements in artificial intelligence approaches, along with power semiconductor devices, have significantly impacted the ability to detect defects in HVDC systems. Furthermore, MATLAB/Simulink is used in the implementation of this developed ANSMA model. After this, the parameters are calculated, and the resulting methodology is tested on an IEEE 50-bus system. Finally, the simulation results are verified using currently used techniques to assess the effectiveness of the suggested ANSMA model.

Keywords: voltage stability; high-voltage direct current system; spider monkey optimization; IEEE bus system

check for updates

Citation: Alsaduni, I. A Novel Security Framework for the Enhancement of the Voltage Stability in a High-Voltage Direct Current System. *Processes* **2023**, *11*, 1028. https://doi.org/10.3390/pr11041028

Academic Editors: Sérgio Ramos and João Soares

Received: 5 January 2023
Revised: 29 January 2023
Accepted: 5 February 2023
Published: 28 March 2023

1. Introduction

In recent years, the development of the HVDC transmission framework has increased throughout the world because of its advantages and uses [1], and the HVDC-based transmission model is utilized in many remote sensing applications [2]. In an HVDC system, line-commutated converters (LCCs) are used [3]. In addition, these kinds of converters are widely utilized for long-distance power connections to provide a power supply [4]. Furthermore, HVDC cross-seam applications require a wide-ranging power supply [5]. In an LCC-based HVDC transmission framework, the power flow usually operates in a unidirectional manner [6]. To change the direction in such a transmission system, the DC line polarity is reversed [7]. In addition, a modified HVDC that is used as a prospective process for cross-seam HVDC applications has been introduced and is based on the method of using line-commutated converters (LCCs) [8]. Normally, HVDC systems are utilized for transmission instead of HVAC models due to their effectiveness, low cost, lower dielectric loss, and lower power loss, which improve the lifetime of a conductor. HVDC connections are created as distinct point-to-point AC/DC interconnections. The existing HVDC systems are differentiated into three models, which are the pole hybrid framework, converter hybrid framework, and terminal hybrid framework. Normally, an HVDC system permits power transmission between AC transmission systems. Furthermore, the power flow is controlled via the phase angle between the source and load. In addition, HVDC converters affect the voltage stability in AC/DC power systems because of their weak voltage stability. In an HVDC system, inverters are needed in the recovery time period, and the minimum time in a negative voltage is attained when an inverter is operated using a particular commutation margin angle. In a power system framework, security measures are important in scheduling generator tasks for long durations [9]. When the voltage stability is good at all levels of load variance, security issues are reduced [10]. However, the major problem in analyzing voltage stability is estimating margin constraints [11]. If margin constraints are not determined, voltage collapse can occur [12]. In addition, system operators often utilize security constraint parameters to decide on an obligation agenda for the generation of components in the future, even if the prediction costs are raised [13]. Moreover, when an electrical load is fulfilled, the commitment choice can meet diverse physical restraints [14], such as minimum down and up durations, generation capability, a reserve ability requirement, a ramping boundary, power stability, and a power transmission flow limit [15].

To diminish transmission failure in power grids, Qi Tao and Yusheng Xue [16] proposed a commutation margin index as a reliable and accurate system to estimate the commutation analysis of a power system. To ensure security, a margin-based security framework was developed in an HVDC system. Moreover, this approach utilized an IEEE 39-bus system for verifying the strength and validity of the developed model. Furthermore, the sensitivity estimation was processed to increase the rapidity of the search process, but it reached an instability range in load variation conditions.

Kaiqi sun et al. [17] developed a novel hybrid system to improve the flexibility and reliability of power flows. Additionally, the flexibility of the system was determined via control procedures that were based on simulation procedures. In addition, the control parameters were analyzed using the proposed model based on the power flow. Finally, the major metrics were compared with existing works, and the effectiveness of the developed model was verified. However, designing the model took more time to complete.

In many cases, voltage instability causes severe security issues by collapsing generation schedule constraints. As such, Ningyu Zhang et al. [18] proposed a voltage stability parameter with security constraints to improve the security measures in a power system. In this model, the voltage stability constraints are considered in a static manner. This technique utilized the Jiangsu power grid and an IEEE 39-bus system in eastern China which involved two or more HVDC transmissions. Finally, key metrics were estimated and compared with other existing works to prove the model's effectiveness. However, this model is complex in design. In modern power systems, an HVDC system is employed to improve the rate of power transmission over long distances in both a controllable and cost-efficient manner. However, the connection of the HVDC system must be carefully evaluated. For this, Enrico M. Carlini et al. [19] proposed a novel transmission network in the HVDC paradigm. Consequently, the performance of the HVDC system was analyzed by measuring its dynamic and steady-state performance. However, in terms of dynamic performance, the proposed system attained a much smaller stability range.

In another study, Bo Zhou et al. [20] proposed a dynamic reserve model to schedule the constraints in using HVDC-based applications. Therein, an even-based model was used to separate the complicated scheduling model to reduce the parameter constraint value and improve the system performance. The proficiency measure of the proposed approach was validated in both normal and disturbance conditions. In the disturbance condition, the developed model attained a much lower stability measure.

In this paper, a novel Adaptive Neural Spider Monkey Algorithm (ANSMA) model is proposed for diminishing the voltage instability in an HVDC system. The proposed model performs functions such as voltage stability enhancement and security enhancement. In this research, an adaptive neural model is combined with spider monkey optimization (SMO) [21], which is capable of enhancing the voltage stability and security of a power system.

In addition, the developed model was compared with recent existing conventional HVDC models such as the hybrid multi-infeed HVDC model (HMIDC) [22], and multivariate random forest regression (MRFR) [23], an optimized power point tracer [24], parabolic optimization [25], reliability assessment [26], an intelligent power tracker [27], the performance of commercial PV [28], a parabolic trough solar power plant [29], etc., but a suitable solution has still not been found. Thus, when the voltage stability is good in all load variance then the security issues get reduced [30,31]. The Coyote Optimization Algorithm (COA) has been successfully used in comparison with other approaches that can be found in the literature to address various optimization problems in numerous fields [32]. The successful decoupling of high-dimensional polynomial nonlinear state-space (PNLSS) models produced a very potent, small model [33]. This operational point's existence and singularity demonstrate that long-term semi-stability may be ensured for any practical power requirement [34]. The arrival of the artificial intelligence era presents a historical opportunity to advance the energy revolution. The development of intelligent energy is the primary indicator of the energy revolution's significant progress since it shows how closely the energy revolution is connected to information technology and industrial technology and how it is gradually maturing. Therefore, the current article aimed to construct a novel hybrid paradigm for a power system using an IEEE bus model to improve security measures. Finally, the proficiency score of the developed model was compared with other works and attained a better stability and scheduling range [35]. A prototype of a smart grid that uses the conservation voltage reduction (CVR) approach to save energy during peak usage hours was created on an Arduino platform. A real-time clock module was used to determine the peak hour, and the zero-cross detection (ZCD) section was used to determine the voltage level [36]. This system is more adaptable than HVDC systems, and the control schemes have grown more sophisticated. Additionally, the stability problems brought on by a decreased system inertia resulting from the ongoing replacement of synchronous machines with HVDC-connected generation are increasingly significant. The limitations of HVDC systems include the switching of mechanical equipment, transmission stability and voltage restrictions, and generator minimum output restrictions. Thus, reducing the cost or loss associated with power generation while maintaining operational and physical constraints is important.

To increase the voltage stability security in an HVDC system, a new method known as ANSMA is created in this work. The ANSMA concept preserves voltage stability when scheduling generator loads. This ANSMA model is implemented using MATLAB/Simulink. The methodology is then tested in an IEEE 50-bus system after the parameters have been determined. Finally, the simulation results are validated using currently used methods to evaluate the efficacy of the proposed ANSMA model. Hence, the novel ANSMA method in this paper is considered a mechanism for enhancing voltage stability.

This paper is arranged as follows: The related works about HVDC systems are detailed in Section 2, and the problem statement and system model are discussed in Section 3. In addition, the process of the developed methodology is detailed in Section 4, and the attained outcomes are elaborated on in Section 5. The conclusion of the proposed work is discussed in Section 6.

2. Literature Survey

Recent Literature Related to HVDC Systems Is Detailed Below

To accomplish both equality and equity, Mozaffari, H. et al. developed the Equal and Equitable Federated Learning (E2FL) [37] innovative collaborative learning algorithm. The authors demonstrated that E2FL beats previous baselines in terms of the resulting efficiency, fairness of distinct groups, and fairness among all individual clients. Furthermore, they validated the efficiency and fairness of E2FL in several real-world federated learning applications.

To assess both fluid density and velocity in various pipe sizes, Roshani et al. created a new intelligent system. Initially, several studies were carried out in dynamic circumstances using the Ba-133 isotope. A static code called Monte Carlo N-Particle extended (MCNPX) was utilized to simulate the setup. The proposed system's mean absolute error (MAE) for calculating density was less than 0.0093. In the experiment, the total standard uncertainty of the fluid average velocity measurement did not surpass 5% [38].

Heterogeneous Private Information Retrieval (HPIR) [39], developed by Mozaffari, H. et al., involves various processing and communication overheads on the part of the PIR servers that implement the protocol. The proposed HPIR algorithms enhance the utility of some of the existing PIR applications and enable new PIR applications via easily transferable parties to engage in managing private services.

Alqudah, A. et al. [40] proposed direct torque control for induction motors by using MATLAB/SIMULINK software, which was employed to introduce a modified fuzzy logic controller with a seven-level diode-clamped inverter and level-shifted carriers-base pulse width modulation (PWM) techniques (which were used to control the multilevel inverter). According to the simulation's findings, the system efficiently regulates motor speed response and improves voltage, current, torque ripple, speed response, and drive performance by lowering the total harmonic distortion (THD) to 6.33%.

To create the optimum hybrid reverse osmosis desalination (ROD) system, life cycle cost (LCC) was examined, along with several continuous and discrete choice variables. M. A. Baseer et al. [41] developed a novel Hybrid Capuchin and Rat Swarm (HCRS) algorithm approach, and the sustainability of the available renewable resources was estimated using the minimization of the LCC, and the desired system reliability was achieved. By using the MATLAB program, experimental studies were carried out, and various parameters were studied and compared with cutting-edge works, which improved the reliability and substantially reduced the LCC.

The objectives and key steps of the proposed work are explained as follows:

- Initially, an IEEE 50-bus system is designed using a MATLAB simulation.
- In addition, a novel Adaptive Neural Spider Monkey Algorithm (ANSMA) is developed to address the voltage stability security issues in HVDC systems.
- The developed ANSMA model is utilized to reduce the generator's agenda with the organization of margin constraints and voltage stability.
- Analysis of the commutation margin index is conducted to improve the security range in power system transmission.
- Subsequently, the proposed model is applied in an IEEE 50-bus system, and several main metrics are measured.
- Finally, the effectiveness of the proposed model is determined by comparing the key metrics with those of existing models in terms of voltage stability, optimal power flow, security range, and so on.

3. System Model and Problem Statement

Preserving security in a power system is a complicated task because of load variance and instability conditions. A loss of voltage stability causes security issues by collapsing the generator scheduling process. Usually, the occurrence of instability occurs in a system because of disturbance, such that when the load varies, the voltage stability is changed. The inability of a power system to meet the demands of reactive power to maintain the preferred voltage in severely stressed systems increases voltage instability. The system model for an HVDC system is represented in Figure 1. Moreover, voltage instability occurs in a system based on the form of the progressive decline in the voltage magnitude at several buses. Voltage instability is the most common difficulty in securing the operation of a power system. In addition, voltage instability for long periods of time can interrupt the power transmission of the system. To address this issue, an efficient neural-based optimization approach for optimal power flow and secure power transmission is designed in this research.

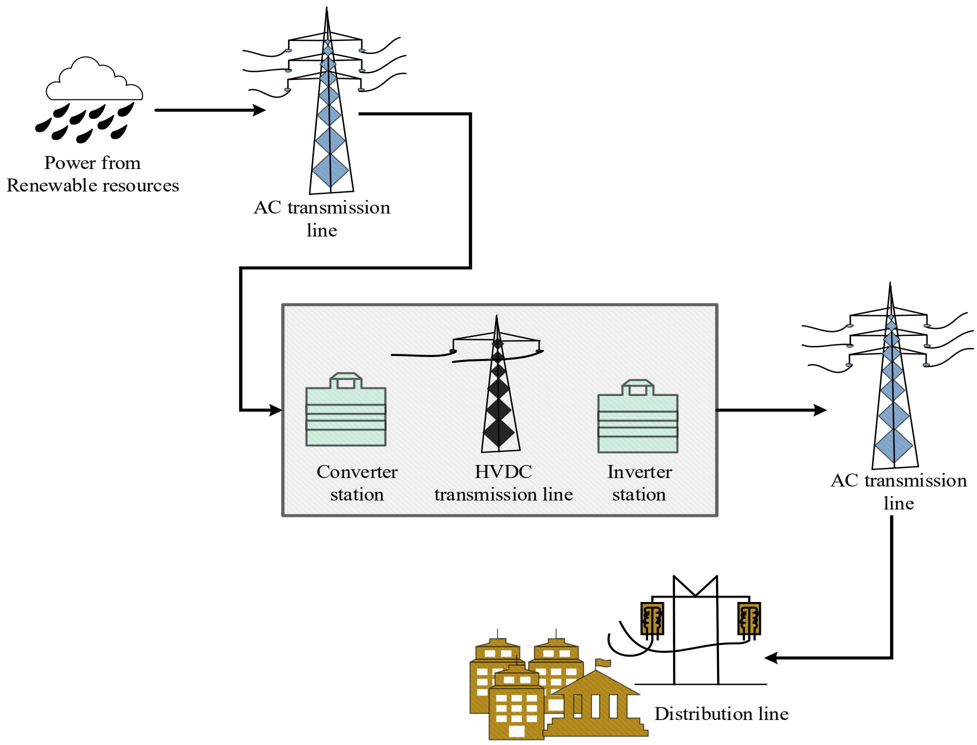

Figure 1. HVDC system model.

Consider the single-line demonstration of a two-bus system that is denoted as k, l bus. Herein, the impedance Z_{kl} from the kth bus to the lth bus is stated in Equation (1):

$$Z_{kl} = R_{kl} + jX_{kl} \tag{1}$$

where R_{kl} and X_{kl} denote the resistance and inductance from the kth bus to the lth bus. In addition, the transmitted and received end voltages are represented as $V_k = Ve^{j\frac{\delta}{2}}$ and $V_l = Ve^{-j\frac{\delta}{2}}$, respectively. Furthermore, the current flow of the single line is calculated using Equation (2):

$$I = \frac{V_k - V_l}{R_{kl} + jX_{kl}} \tag{2}$$

Additionally, the real power P_{kl} and reactive power Q_{kl} on the transmitting as well as receiving side with angle $\Phi = \tan^{-1}(\frac{P_l}{Q_l})$ are computed using Equations (3) and (4):

$$P_{kl} = V_l \left[\frac{V_k - V_l}{R_{kl} + jX_{kl}} \right] \cos\phi \tag{3}$$

$$Q_{kl} = V_l \left[\frac{V_k - V_l}{R_{kl} + jX_{kl}} \right] \sin\phi \tag{4}$$

The equality constraints of the real and reactive power are calculated using Equations (5) and (6) for each bus with the time period T:

$$P_{gk}^T - P_{hk}^T - V_k^T \sum_{l=1}^{n} V_l^T \left(B_{kl}^c \cos\theta_{kl}^T + g_{kl} \sin\theta_{kl}^T \right) = 0; (k = 1, 2, 3, \ldots\ldots\ldots\ldots n) \tag{5}$$

$$Q_{gk}^T - Q_{hk}^T - V_k^T \sum_{l=1}^{n} V_l^T \left(B_{kl}^c \sin\theta_{kl}^T + g_{kl} \cos\theta_{kl}^T \right) = 0; (k = 1, 2, 3, \ldots\ldots\ldots\ldots n) \tag{6}$$

where $P^T{}_{gk}$ and $Q^T{}_{gk}$ represent the active and reactive power that are produced at the bus k, l with time period T; $P^T{}_{hk}$ and $Q^T{}_{hk}$ denote the requirements of active and reactive power; V_k and V_l are the magnitudes of the voltage; g_{kl} is the susceptance and $B^C{}_{kl}$ is the conductance between the buses k and l; n denotes the number of buses; and $\theta^T{}_{kl}$ is the voltage of the phase angle between the buses k and l with time period T.

Additionally, the inequality constraints of the real and reactive power generator are expressed in Equations (7) and (8):

$$P_{gk}^{\min} \leq P_{gk} \leq P_{gk}^{\max}(k = 1, 2, 3, \ldots\ldots, g_n) \tag{7}$$

$$Q_{gk}^{\min} \leq Q_{gk} \leq Q_{gk}^{\max}(k = 1, 2, 3, \ldots\ldots, g_n) \tag{8}$$

where $P^{min}{}_{gk}$ and $Q^{min}{}_{gk}$ denote the minimum boundaries of the real and reactive power in the bus k, and g_n represents the generator bus.

4. Proposed ANSMA Methodology

Maintaining the security of a power system is a challenging task due to load variations and voltage instability conditions. The key focus of this research is to enhance a power system by securing an IEEE bus system. Therefore, a novel Adaptive Neural Spider Monkey Algorithm (ANSMA) was developed in an IEEE bus system to reduce the scheduling issues in the generator with security constraints and voltage stability.

Voltage stability improves the security of a power system under any load changes. The power system's communication performance was evaluated using the commutation margin index to expand the security range. The proposed architecture is shown in Figure 2.

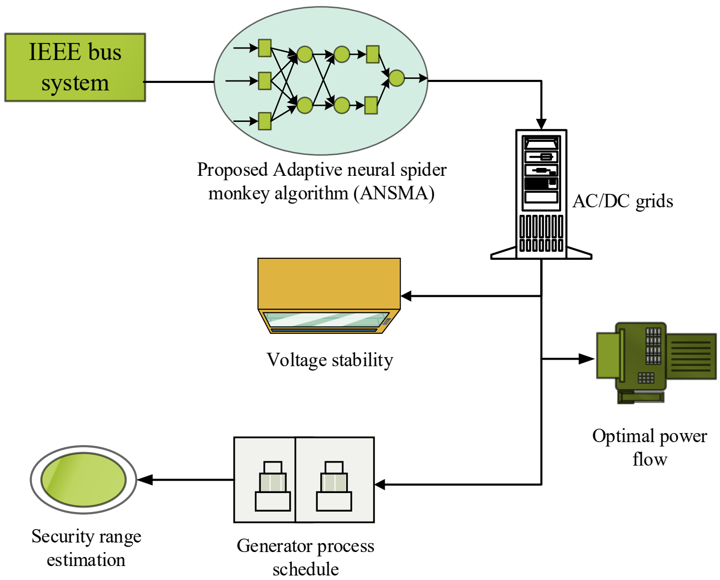

Figure 2. Diagram of proposed ANSMA.

ANSMA Model for Voltage Stability

This optimization model is widely utilized in the power system to minimize undesirable influences and maximize essential influences that can help to accomplish best-optimized results under numerous constraints. Initially, the attained parameters from the IEEE bus (k) system, such as bus voltage V_k, load angle L_φ, real power P_k, and reactive power Q_k, are given to the input layer of the network. The data initialization process using the ANSMA model in the input layer is detailed in Equation (9):

$$bv*_k = V_{k_{\min}} + U(0,1) \times L_n\phi\left(V_{k_{\max}} - V_{k_{\min}}\right)(P_k, Q_k) \tag{9}$$

where $V_{k\,min}$ and $V_{k\,max}$ denote the minimum and maximum levels of bus voltage in the k^{th} bus, and U(0, 1) denotes a random number uniformly distributed in the range (0, 1). The fitness function of the model is expressed in Equation (10), which is utilized as the stability margin of the bus. In addition, the stability margin is defined as the variance between the operating load level and the load ability level. The process of the ANSMA network model is represented in Figure 3.

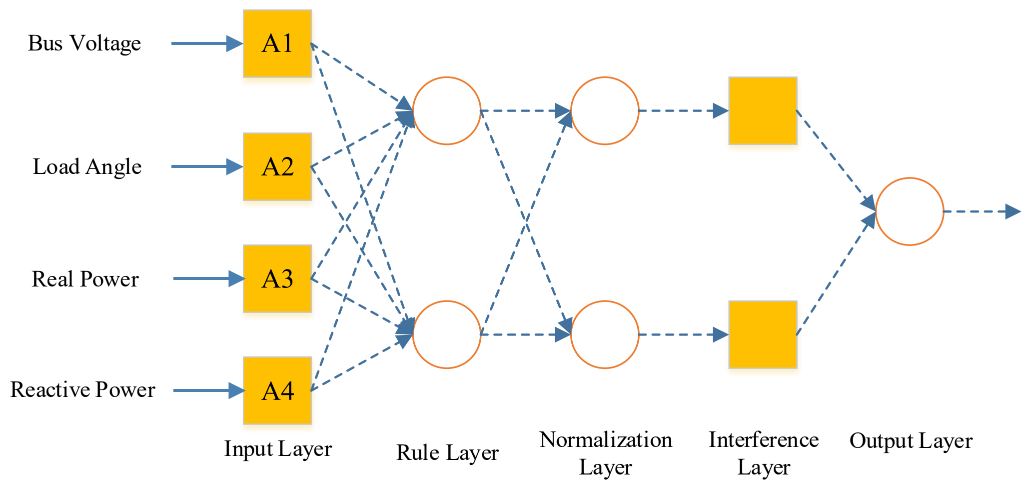

Figure 3. Process of ANSMA model.

The decisions are selected in the rule layer of the network that is processed using the ANSMA model. In addition, the voltage stability margin is calculated using Equation (10):

$$R_k = \begin{cases} S_{Vk}\ 0 < V \geq 1 \\ I_{Vk}\ V < 1 \end{cases} \tag{10}$$

where S_{Vk} denotes the voltage stability, and I_{Vk} denotes the voltage instability condition. Herein, the utilized voltage level in each line is calculated, and that which has levels of less than 1 V is considered as voltage stability. Furthermore, if the voltage level is greater than 1 V, it is considered as voltage instability. Moreover, voltage stability is increased based on the planning, maintenance, and operation of a generation system. Consequently, voltage stability is enhanced using Equation (11):

$$\text{Prob}V_k = \frac{R_k}{\sum_{k=1}^{g_n} R_k \delta_L}(g_M) \tag{11}$$

where R_k denotes the voltage stability margin, δ_L represents the load reduction factor for improving voltage stability, and g_M represents the generation of the maintaining factor.

- Load scheduling

Load scheduling is necessary for the electrical design activities that provide the earliest details about the process, load arrangement, and building. Initially, a list of predictable electrical loads is collected, and for every load, the electrical parameters are collected.

$$S_L = CL_n\{V_{kl} + U(0,1) + (\varphi * R_{kl} * e_{kl})\} \tag{12}$$

Here, S_L and CL_n denote the load scheduling and the classification of n number of loads based on the location and duty of the loads. Furthermore, ϕ denotes the angle between the loads, and e_{kl} denotes the electrical parameters that include power factor, efficiency, and nominal/observed ratings. This load scheduling process is utilized for arranging the generators.

- Enhanced Voltage Stability

Network reconfiguration in a radial distribution system is accomplished by closing the tie and sectionalizing switches. However, this can result in an impractical setup, either by creating a closed loop or omitting one or more branches from the arrangement. This can be prevented by carefully controlling the connectivity from the source to all the nodes during the network reconfiguration. The state of each switch in a switch group is realized for each switching combination. While the configurations for left-connect or right-connect vary in accordance with the logic of the left- or right-connect, zero-connect sees no change in configuration. Utilizing the power flow in the tie branch's adjacent branches, a left- and right-connect logic is established in the system. When the system is reconfigured, the power flow in the open branch, which was flowing prior to reconfiguration, moves to the newly linked tie branch by closing the tie branch and opening either of the adjoining branches. The power flow in the right branch of the tie branch switches to the tie branch if the left-connect is executed.

Finally, simulations suggest that installing a battery at the load substation to inject the right amount of reactive and active power can enhance a system's voltage stability. Low voltages are frequently a reliable indicator of the areas where load shedding would be helpful for reducing system stress. Load shedding is reduced by minimizing the unnecessary usage and charging of electrical appliances.

- Voltage security margin (VSM)

Voltage security is a serious problem in power systems that occurs when voltage instability arises in the system. Voltage instability is increased due to variations in the loads. The proposed approach utilizes the static voltage stability margin (VSM) for evaluating voltage security in the power grid, and the VSM represents the boundary between the secure and insecure voltage areas.

The process of the proposed ANSMA model is elaborated in Algorithm 1 and represented in Figure 4.

Algorithm 1: ANSMA for voltage stability

Start
{
Create the IEEE 50 bus
Initialize the input parameters V_k, L_φ, P_k, and Q_k ***//bus voltage, load angle, real power, and reactive power***
Input parameters are trained to the system
Calculate the stability margin
    If $0 < V \geq 1.1$ ***then*** S_{vij} ***//voltage stability***
    Else
    Voltage instability
    End if
Voltage stability improvement()
    For all(k)
    Consider $\boldsymbol{R_k}$ ***//voltage stability margin***
    Calculate $\mathrm{ProbV_k}$
    End for
Load scheduling()
    For all(k)
    Consider the variation in loads
    Identify the location, electrical parameters, and angle of the loads
    Calculate S_L *using Equation (12)* ***//load scheduling***
    End for
Voltage security margin()
    If *high voltage stability*
    Then
    High security
    End if
Optimal outcomes ***//(voltage stability, power flow, and high security)***
}
Stop

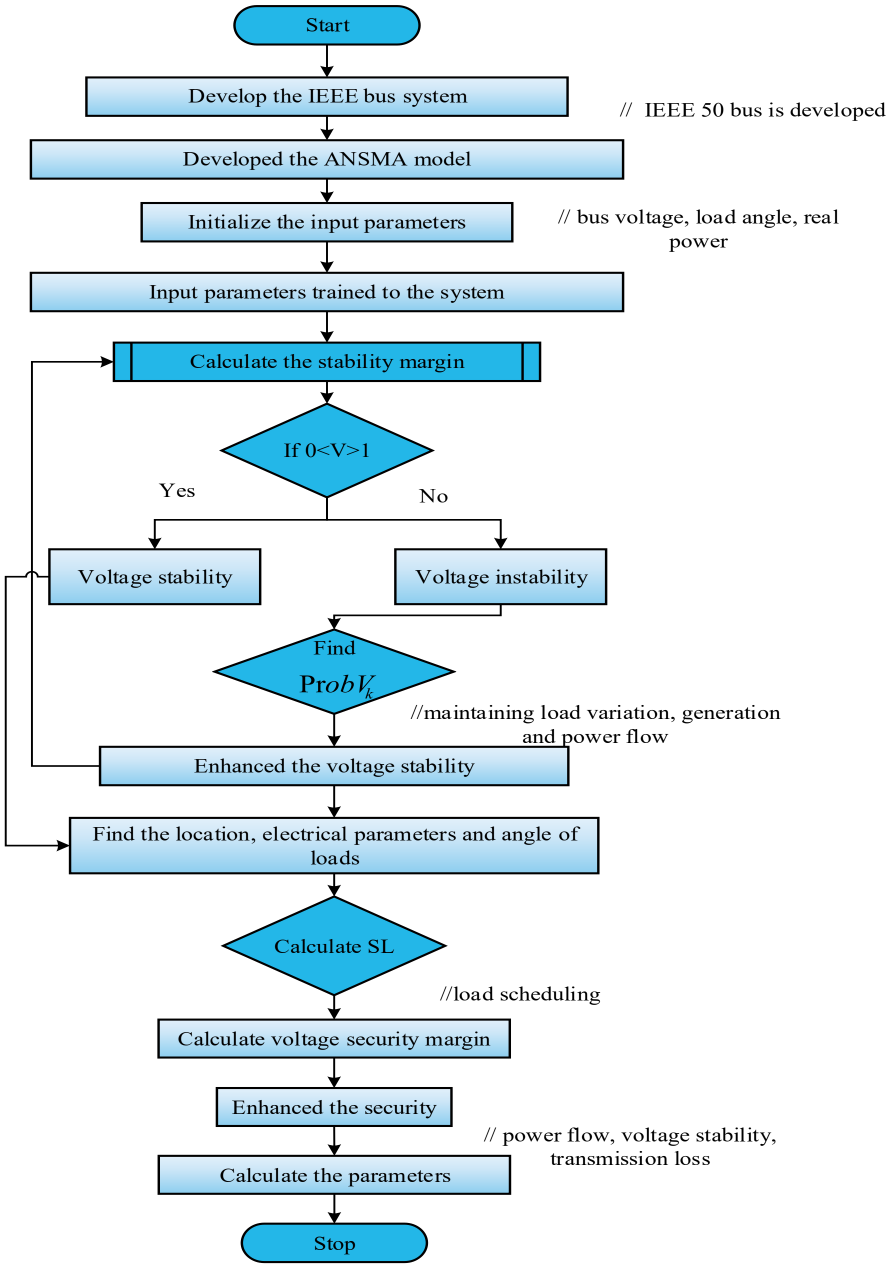

Figure 4. Flowchart representation of the proposed ANSMA model.

5. Result and Discussion

The developed ANSMA model was implemented and simulated using MATLAB/Simulink R2018b in Intel (R) Core (TM) i5 pro along with a 4 GB RAM. In this research, the main aim was to attain the optimal power flow, high stability, and the VSM. Herein, the outcomes of the projected model are evaluated in terms of voltage stability under different load conditions, transmission loss, optimal power flow, security range, and real and reactive power. Furthermore, the performance of the proposed model is compared with existing approaches for validating the efficiency of the proposed ANSMA model.

5.1. Case Study for IEEE 50-Bus System

The proposed ANSMA approach is mainly utilized in an HVDC system for enhancing voltage stability and security. In this study, an IEEE 50-bus system model was designed for evaluating the performance of the system. Primarily, input parameters such as load angle $L\varphi$, real power P_k, reactive power Q_k, and bus voltage V_k were considered for the IEEE 50-bus system, and these input variables are initialized using Equation (9). The IEEE 50-bus system involves 10 synchronous generators and 2 HVDC transmissions, which are illustrated in Figure 5. Therein, the utilized generators are denoted as G41 to G50 and two HVDC transmissions. Herein, the HVDC transmission capacities are considered as 1000 MW, and the generator capacity of the system is considered as 4800 MW. Additionally, the stability margin of the proposed model is calculated using Equation (10). In this equation, the voltage level of the generator is considered as $0 < V \geq 1.1$. If the voltage level is lower than 1.1 V, it is considered as stable voltage; otherwise, it is unstable. Thus, the proposed model calculates the voltage level and enhances the voltage stability using Equation (11) while maintaining the loads and generators. In this model, the load scheduling process is carried out using Equation (12) based on the location of loads that are employed to arrange the generators in the IEEE 50-bus system. When the voltage stability is maintained, the security of the system is improved. In this IEEE 50-bus system, the inner HVDC model and the exterior power source are utilized to attain a dynamic load center. The smallest VSM of the local power grid is larger than the normal operation of the power grid because of the technical specifications for system security and voltage stability.

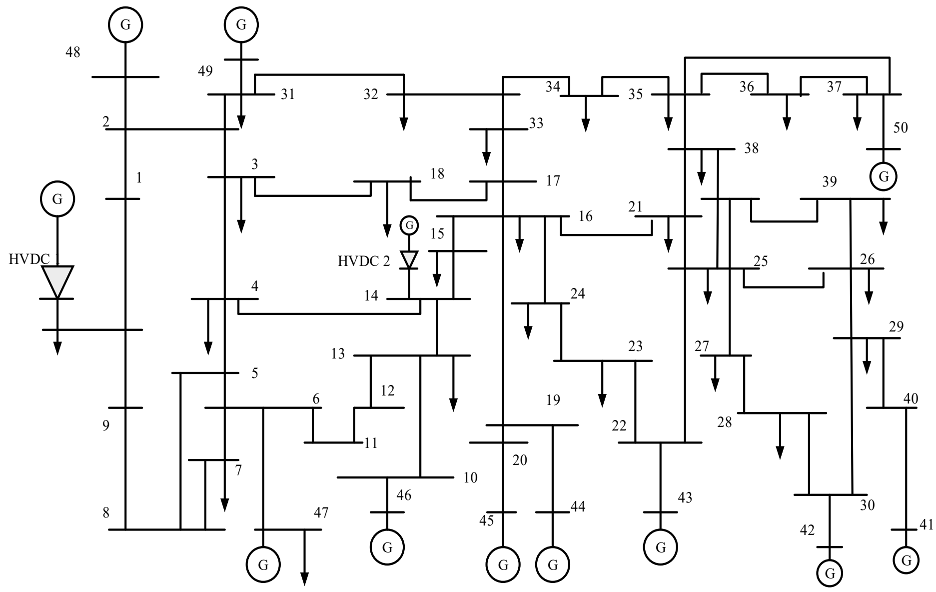

Figure 5. IEEE 50-bus system.

The model was then applied to two cases: a system without security constraints and VSM constraints and a system with the proposed ANSMA security constraints and VSM constraints. The designed IEEE 50-bus system has 10 generators that use various loads. When compared with conventional HVDC models, the suggested ANSMA technique achieves excellent security and stability while offering optimal power flow values. The base voltage of the proposed model is considered as 1.1 V. Voltage profiles of the functions including voltage deviation, power loss, and generation cost are illustrated in Figure 6.

The power loss convergence curve of the designed IEEE 50-bus system was compared with the existing models, which are represented in Figure 7. The proposed ANSMA model achieved a lower power loss compared with other models, including HMIDC, MRFR, and hybrid grid. The calculation of the power loss for the IEEE 50-bus system using the proposed ANSMA approach was compared with the existing methods, which are illustrated in Figure 7. The power loss should be minimal in an efficient bus system, but the existing approaches exhibited high power losses. Thus, the proposed ANSMA model attained a lower power loss than the other conventional models.

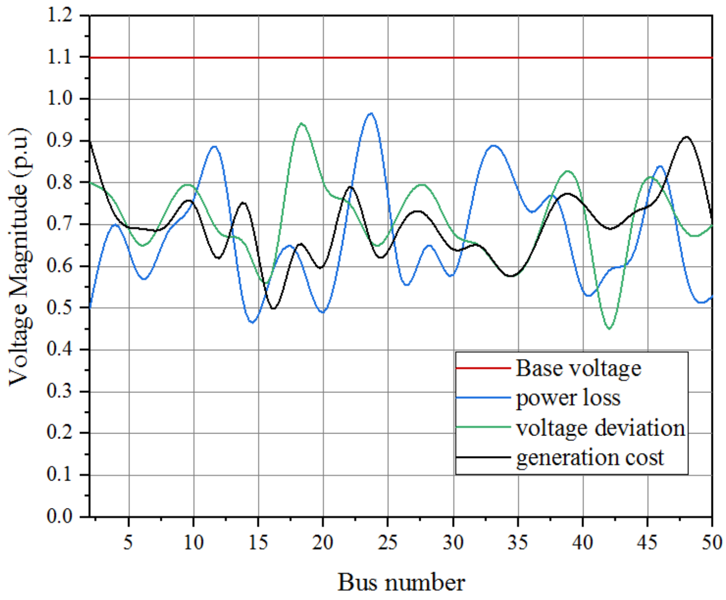

Figure 6. Voltage profiles of IEEE 50-bus system.

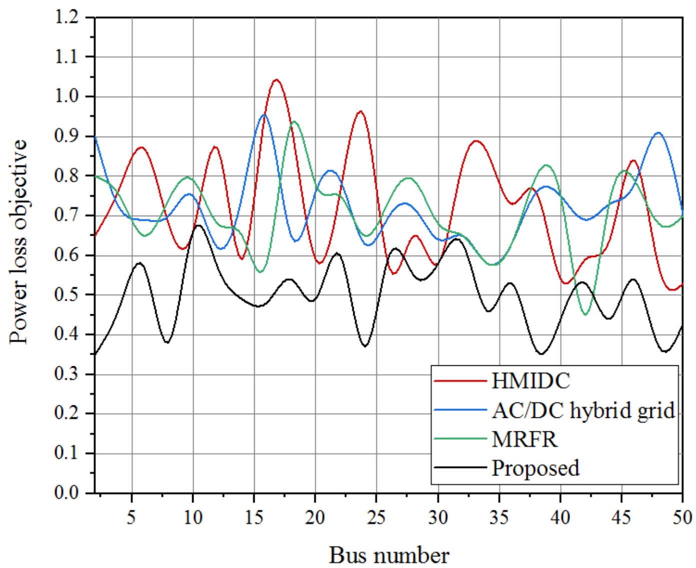

Figure 7. Convergence curves for power loss of IEEE 50-bus system.

The calculation of the voltage deviation convergence curve for the IEEE 50-bus system using the proposed ANSMA approach was compared with existing methods, which are illustrated in Figure 8. The voltage deviation should be minimal in an efficient bus system, but the existing approaches demonstrated high voltage deviations. Thus, the proposed ANSMA model attained a lower voltage deviation than the other conventional models.

The convergence curves for the generation costs of the IEEE 50-bus system comparisons are represented in Figure 9. The proposed model attained a lower generation cost for the IEEE 50-bus system than the other approaches. The ANSMA model's two main goals are either minimizing manufacturing costs or increasing production efficiency. Herein, minimization of the generation cost is the major criterion used by the ANSMA model. Therefore, compared with the other current techniques, the developed ANSMA model achieved lower power loss and generation cost.

The proposed model utilized optimal power and voltage in the IEEE 50-bus system. The active power and reactive power utilizations of the bus system generators are calculated and detailed in Table 1. Normally, active power is defined as the product of current (I) and voltage (V), and the cosine and sine of the angle between these values are defined as the reactive power. Moreover, existing methods including HMIDC, the AC/DC hybrid grid, and MRFR approaches utilize high power values. Thus, the proposed model attained optimal power flow in the IEEE bus system.

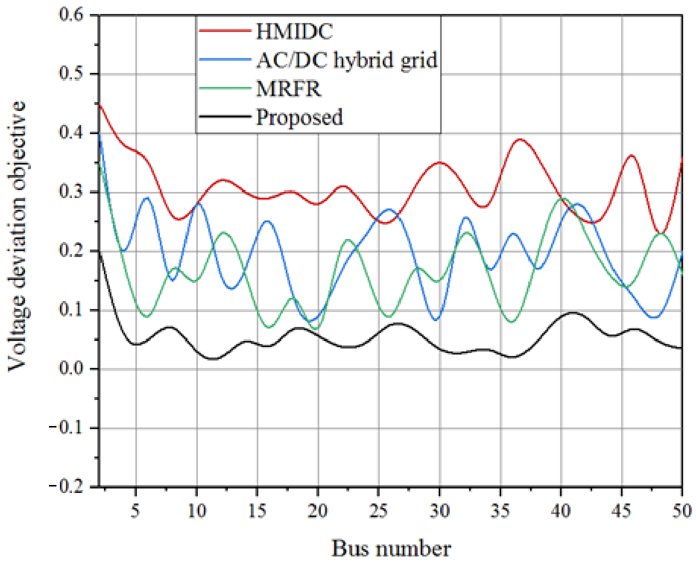

Figure 8. Convergence curves for voltage deviation of IEEE 50-bus system.

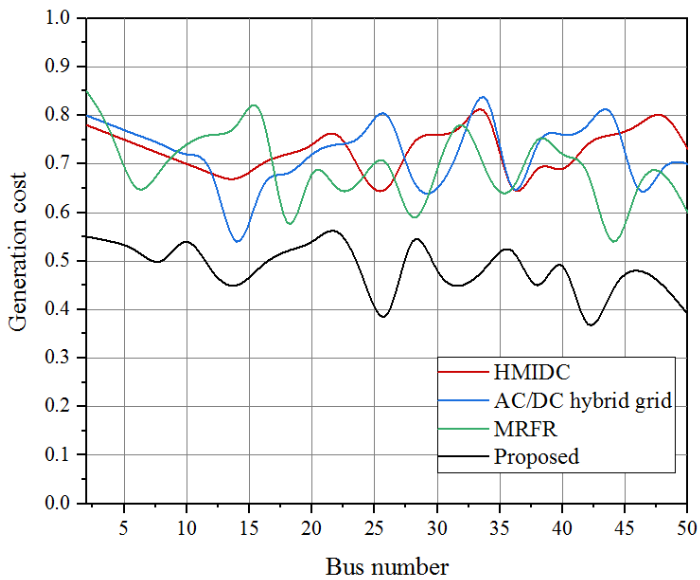

Figure 9. Convergence curves for generation cost of IEEE 50-bus system.

The voltage usage values of the bus system generators are calculated and detailed in Table 2. It can be observed that the existing methods such as HMIDC, the AC/DC hybrid grid, and MRFR approaches utilize high voltage values. Thus, the proposed model attained optimal voltage levels in the IEEE bus system.

Table 1. Performance comparison of power flow of the proposed ANSMA model with those of existing methods in IEEE 50-bus system.

Main Objective Functions and Variables	HMIDC [22]	AC/DC Hybrid Grid [18]	MRFR [23]	Proposed (ANSMA)
P_{G41} (MW)	210.7	155.1242	145.345	130.56
P_{G42} (MW)	100	77.6136	126.667	120.45
P_{G43} (MW)	127.56	19.6631	107.45	56.69
P_{G48} (MW)	27	34.7131	54.78	46.35
P_{G50} (MW)	30	30.032	34.78	27.45
Q_{G41} (VAR) (p.u)	825	670	850	430
Q_{G42} (VAR) (p.u)	355	540	430	150
Q_{G43} (VAR) (p.u)	257	375	260	55
Q_{G48} (VAR) (p.u)	737	420	175	78
Q_{G50} (VAR) (p.u)	250	125	270	32
P_{conv} (in p.u)	-	1.0765	1.1	1.023
Power loss (MW)	17.56	24.5	36.67	10.67
Cost (USD/hr)	3759	456.25	765.50	207.46
Time (s)	45	60	55	15

Table 2. Performance comparison of voltage deviation of the proposed ANSMA model with those of existing methods in IEEE 50-bus system.

Main Objective Functions and Variables	HMIDC [22]	AC/DC Hybrid Grid [18]	MRFR [23]	Proposed (ANSMA)
V_{41} (*in p.u*)	1.3	1.0835	1.0765	1.0693
V_{42} (*in p.u*)	1.05	1.0835	1.0765	1.0877
V_{43} (*in p.u*)	1.01	0.9811	1.0724	1.0263
V_{48} (*in p.u*)	1.1	1.0724	1.0656	1.036
V_{50} (*in p.u*)	1.03	1.0639	1.035	1.062
V_{dc} (*in p.u*)	-	1.0852	1.045	1.0831

The proposed ANSMA approach required a lower computation time and cost for designing the IEEE 50-bus system in the HVDC model. The computation time and cost of the proposed model are compared with those of the existing approaches and are represented in Figure 10.

5.2. Discussion

The proposed model attained better results than the other models in terms of power flow, security, and voltage stability. The comparison of the state-of-the-art approaches with the proposed model is elaborated in Table 3.

The developed model attained optimal power flow, high security, and high stability in the IEEE 50-bus system compared with the other models.

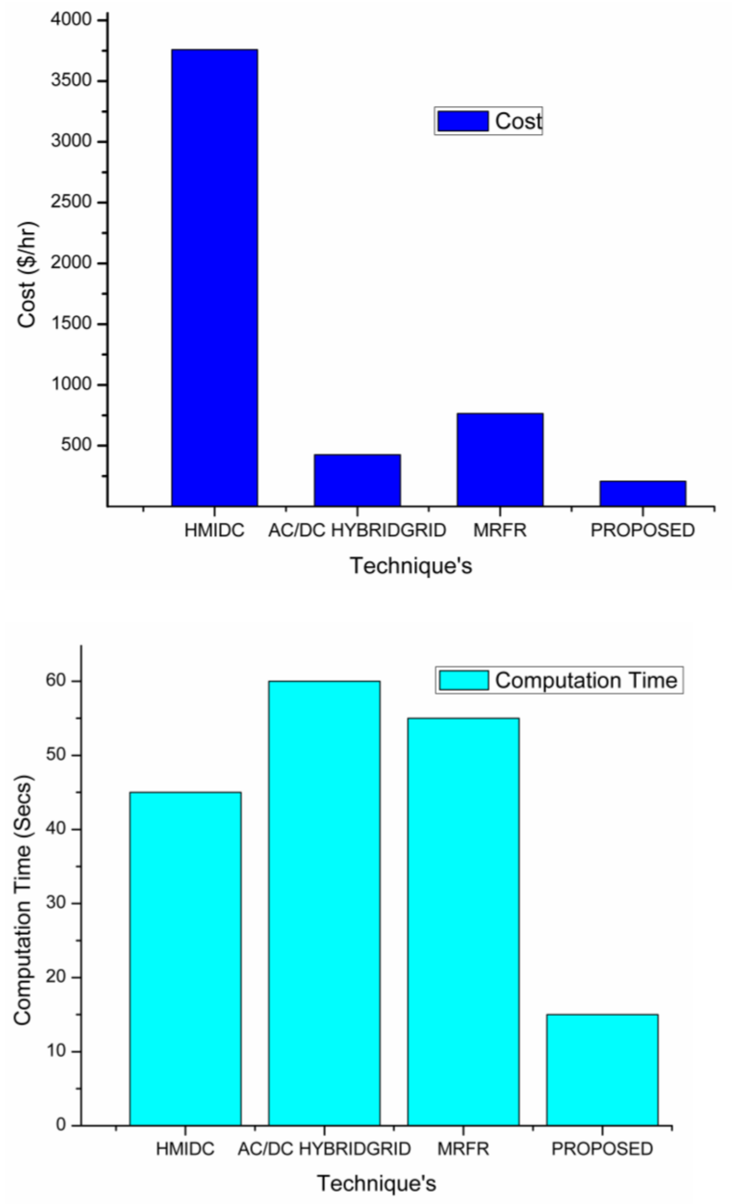

Figure 10. Comparison of computation times and costs.

Table 3. State-of-the-art methods compared with proposed method.

Author	Method	Advantages	Disadvantages
Qi Tao and Yusheng Xue [16]	Margin-based security frame	Enhance the security	Instability range in load variation condition
Kaiqi sun et al. [17]	Hybrid systems	Improve the flexibility and reliability of power flows	Designing the model takes more time to complete
Ningyu Zhang et al. [18]	Hybrid grid	Enhance the security of IEEE 39-bus system	This model is complex and takes more time to design
Enrico M. Carlini et al. [19]	Transmission network in HVDC	Dynamic and steady state performance	Very small stability range
Bo Zhou et al. [20]	Dynamic reserve model	Reduce the parameter constraints	Very little measured stability
Proposed	ANSMA	Optimal power flow, high security, and high stability in the IEEE 50-bus system	-

6. Conclusions

In this research, a novel Adaptive Neural Spider Monkey Algorithm (ANSMA) model was developed for enhancing voltage stability and security in an HVDC system. The developed ANSMA model was applied to an IEEE 50-bus system. The voltage stability was enhanced by scheduling the loads in the generator that was analyzed using the IEEE 50-bus system. Moreover, the improvement in the voltage stability in the bus system was increased from 1.045 p.u to 1.0831 p.u, as was the security of the HVDC system. Additionally, the performance of the proposed model was analyzed based on the power flow, voltage stability, and security range. It was observed that the proposed ANSMA approach attained high voltage stability and optimized power flow. In the proposed system, the power loss was reduced from 36.67 MW to 10.67 MW, and the cost gradually decreased from 765.50 USD/h to 207.46 USD/h. Thus, the developed model attained reduced power losses and generation costs compared with the other prevailing approaches.

Funding: This research was supported by the Deanship of Scientific Research, Majmaah University, Al-Majmaah-11952, Kingdom of Saudi Arabia, under project number R-2023-15.

Data Availability Statement: The data analyzed in this study are provided in the paper.

Conflicts of Interest: The authors declare no conflict of interest.

References

1. Liu, D.; Li, Z.; Xu, H. HVDC Commutation Failures Detection for Security and Stability Control Based on Local Electrical Quantities. In Proceedings of the PURPLE MOUNTAIN FORUM 2019-International Forum on Smart Grid Protection and Control; Lecture Notes in Electrical Engineering. Springer: Singapore, 2020; pp. 247–255. [CrossRef]
2. Elgamasy, M.M.; Taalab, A.-M.I.; Kawady, T.A.; Izzularab, M.A.; Elkalashy, N.I. Wave propagation differential protection scheme for VSC-HVDC transmission systems. *Electr. Power Syst. Res.* **2020**, *189*, 106826. [CrossRef]
3. Linke, F.; Alhomsi, H.; Westermann, D. Investigation of the critical fault clearing time in HVDC-systems on the angle stability of generators in the AC system using protection zones. In Proceedings of the NEIS 2020 Conference on Sustainable Energy Supply and Energy Storage Systems, Hamburg, Germany, 14–15 September 2020.
4. Yan, Y.; Sun, N.; Zhang, N.; Zhao, H.; Li, S. Hierarchical Reliability Evaluation to Security and Stability Control System of Power Systems. In Proceedings of the 2020 5th Asia Conference on Power and Electrical Engineering (ACPEE), Chengdu, China, 4–7 June 2020.
5. Sennewald, T.; Linke, F.; Westermann, D. Preventive and Curative Actions by Meshed Bipolar HVDC-Overlay-Systems. *IEEE Trans. Power Deliv.* **2020**, *35*, 2928–2936. [CrossRef]
6. Chen, B.; Yim, S.-I.; Kim, H.; Kondabathini, A.; Nuqui, R. Cybersecurity of Wide Area Monitoring, Protection and Control Systems for HVDC Applications. *IEEE Trans. Power Syst.* **2020**, *36*, 592–602. [CrossRef]
7. Wu, X.; Xiao, L.; Yang, J.; Xu, Z. Design method for strengthening high-proportion renewable energy regional power grid using VSC-HVDC technology. *Electr. Power Syst. Res.* **2019**, *180*, 106160. [CrossRef]
8. Jiang, T.; Zhang, R.; Li, X.; Chen, H.; Li, G. Integrated energy system security region: Concepts, methods, and implementations. *Appl. Energy* **2020**, *283*, 116124. [CrossRef]
9. Wu, C.; Zhang, D.; He, J. A Novel Protection Scheme for MMC-HVDC Transmission Lines Based on Cross-Entropy of Charge. *IEEE Access* **2020**, *8*, 222800–222812. [CrossRef]
10. Zhu, Z.; Yan, J.; Lu, C.; Chen, Z.; Tian, J. Two-Stage Coordinated Control Strategy of AC/DC Hybrid Power System Based on Steady-State Security Region. *IEEE Access* **2020**, *8*, 139221–139243. [CrossRef]
11. Abbasipour, M.; Milimonfared, J.; Yazdi, S.S.H.; Rouzbehi, K. Power injection model of IDC-PFC for NR-based and technical constrained MT-HVDC grids power flow studies. *Electr. Power Syst. Res.* **2020**, *182*, 106236. [CrossRef]
12. Cheng, J.; Dou, F.; Wang, W.; Le, X.; Zhen, H. Regional Generator Excitation Control Strategy for HVDC Commutation Failure Suppression. In Proceedings of the 2020 12th IEEE PES Asia-Pacific Power and Energy Engineering Conference (APPEEC), Nanjing, China, 20–23 September 2020.
13. Wang, J.; Xu, Q.; Dai, P.; Xin, H. A Recovery Method for HVDC Systems Following AC System Faults. In Proceedings of the 2020 IEEE/IAS Industrial and Commercial Power System Asia (I&CPS Asia), Weihai, China, 13–15 July 2020.
14. Glende, E.; Wolter, M. Tracing HVDC Flows using the proportional sharing principle. In Proceedings of the 2020 IEEE PES Innovative Smart Grid Technologies Europe (ISGT-Europe), The Hague, The Netherlands, 26–28 October 2020.
15. Musca, R.; Bizumic, L. Primary Frequency Control in the Power System of Continental Europe including the Dynamics of the HVDC Link France-Great Britain. In Proceedings of the 2020 AEIT International Annual Conference (AEIT), Catania, Italy, 23–25 September 2020.

16. Tao, Q.; Xue, Y. Quantitative Assessment for Commutation Security Based on Extinction Angle Trajectory. *J. Mod. Power Syst. Clean Energy* **2021**, *9*, 328–337. [CrossRef]
17. Sun, K.; Xiao, H.; Pan, J.; Liu, Y. A Station-Hybrid HVDC System Structure and Control Strategies for Cross-Seam Power Transmission. *IEEE Trans. Power Syst.* **2020**, *36*, 379–388. [CrossRef]
18. Zhang, N.; Wu, S.; An, H.; Zhu, X. Security-Constraint Unit Commitment for AC/DC Transmission Systems with Voltage Stability Constraint. *J. Electr. Eng. Technol.* **2020**, *15*, 2459–2469. [CrossRef]
19. Carlini, E.M.; Vergine, C.; Gadaleta, C.; Aluisio, B.; Migliori, M.; Dicorato, M.; Trovato, M.A.; Forte, G. Static and dynamic evaluation of different architectures for an actual HVDC link project. *IEEE Trans. Power Deliv.* **2020**, *35*, 2782–2790. [CrossRef]
20. Zhou, B.; Fang, J.; Ai, X.; Yang, C.; Yao, W.; Wen, J. Dynamic Var Reserve-Constrained Coordinated Scheduling of LCC-HVDC Receiving-End System Considering Contingencies and Wind Uncertainties. *IEEE Trans. Sustain. Energy* **2020**, *12*, 469–481. [CrossRef]
21. Akhand, M.; Ayon, S.I.; Shahriyar, S.; Siddique, N.; Adeli, H. Discrete Spider Monkey Optimization for Travelling Salesman Problem. *Appl. Soft Comput.* **2019**, *86*, 105887. [CrossRef]
22. Li, D.; Sun, M.; Fu, Y. A General Steady-State Voltage Stability Analysis for Hybrid Multi-Infeed HVDC Systems. *IEEE Trans. Power Deliv.* **2020**, *36*, 1302–1312. [CrossRef]
23. Sun, K.; Xiao, H.; Liu, S.; Liu, Y. A machine learning-based fast frequency response control for a VSC-HVDC system. *CSEE J. Power Energy Syst.* **2020**, *7*, 688–697.
24. Abdul Baseer, M.; Almunif, A.; Alsaduni, I.; Zubair, M.; Tazeen, N. An adaptive power point tracker in wind photovoltaic system using an optimized deep learning framework. *Energy Sources Part A Recovery Util. Environ. Eff.* **2022**, *44*, 4846–4861. [CrossRef]
25. Zubair, M.; Awan, A.B.; Baseer, M.A.; Khan, M.N.; Abbas, G. Optimization of parabolic trough based concentrated solar power plant for energy export from Saudi Arabia. *Energy Rep.* **2021**, *7*, 4540–4554. [CrossRef]
26. Baseer, M.A.; Alsaduni, I.; Zubair, M. A Novel Multi-Objective Based Reliability Assessment in Saudi Arabian Power System Arrangement. *IEEE Access* **2021**, *9*, 97822–97833. [CrossRef]
27. Abdul Baseer, M.; Alsaduni, I.; Zubair, M. Novel hybrid optimization maximum power point tracking and normalized intelligent control techniques for smart grid linked solar photovoltaic system. *Energy Technol.* **2021**, *9*, 2000980. [CrossRef]
28. Baseer, M.; Praveen, P.R.; Zubair, M.; Khalil, A.G.A.; Al Saduni, I. Performance and Optimization of Commercial Solar PV and PTC Plants. *Int. J. Recent Technol. Eng.* **2020**, *8*, 1703–1714. [CrossRef]
29. Praveen, P.R.; Awan, A.B.; Zubair, M.; Baseer, M.A. Performance Analysis and Optimization of a Parabolic Trough Solar Power Plant in the Middle East Region. *Energies* **2018**, *11*, 741. [CrossRef]
30. Jeeninga, M.; De Persis, C.; Van der Schaft, A. DC power grids with constant-power loadsPart I: A full characterization of power flow feasibility, long-term voltage stability and their correspondence. *IEEE Trans. Autom. Control* **2022**, *68*, 2–17. [CrossRef]
31. Wang, X.; Wu, H.; Wang, X.; Dall, L.; Kwon, J.B. Transient Stability Analysis of Grid-Following VSCs Considering Voltage-Dependent Current Injection during Fault Ride-through. *IEEE Trans. Energy Convers.* **2022**, *37*, 2749–2760. [CrossRef]
32. Meraihi, Y.; Gabis, A.B.; Ramdane-Cherif, A.; Acheli, D. Advances in Coyote Optimization Algorithm: Variants and Applications. In *Advances in Computational Intelligence and Communication*; Springer: Cham, Switzerland, 2023; pp. 99–113.
33. Csurcsia, P.Z.; Decuyper, J.; Renczes, B.; De Troyer, T. Nonlinear Modelling of an F16 Benchmark Measurement. In *Nonlinear Structures & Systems*; Springer: Cham, Switzerland, 2023; Volume 1, pp. 49–60.
34. Gao, J.; Chen, S.; Li, X.; Zhang, J. Transient Voltage Control Based on Physics-Informed Reinforcement Learning. *IEEE J. Radio Freq. Identif.* **2022**, *6*, 905–910. [CrossRef]
35. Mohamed, M.A.E.; Mohamed, S.M.R.; Saied, E.M.M.; Elsisi, M.; Su, C.-L.; Hadi, H.A. Optimal Energy Management Solutions Using Artificial Intelligence Techniques for Photovoltaic Empowered Water Desalination Plants under Cost Function Uncertainties. *IEEE Access* **2022**, *10*, 93646–93658. [CrossRef]
36. Rahman, M.M.; Saha, S.; Majumder, M.Z.H.; Suki, T.T.; Akter, F.; Haque, M.A.S.; Hossain, M.K. Energy Conservation of Smart Grid System Using Voltage Reduction Technique and Its Challenges. *Evergreen* **2022**, *9*, 924–938. [CrossRef]
37. Mozaffari, H.; Houmansadr, A. E2FL: Equal and Equitable Federated Learning. *arXiv* **2022**, arXiv:2205.10454.
38. Roshani, G.H.; Hanus, R.; Khazaei, A.; Zych, M.; Nazemi, E.; Mosorov, V. Density and velocity determination for single-phase flow based on radiotracer technique and neural networks. *Flow Meas. Instrum.* **2018**, *61*, 9–14. [CrossRef]
39. Mozaffari, H.; Houmansadr, A. Heterogeneous private information retrieval. In Proceedings of the Network and Distributed Systems Security (NDSS) Symposium, San Diego, CA, USA, 23–26 February 2020.
40. Alqudah, A.; Mohaidat, M.; Altawil, I. Control of variable speed drive (VSD) based on diode clamped multilevel inverter using direct torque control and fuzzy logic. In Proceedings of the 2013 IEEE Jordan Conference on Applied Electrical Engineering and Computing Technologies (AEECT), Amman, Jordan, 3–5 December 2013.
41. Baseer, M.A.; Kumar, V.V.; Izonin, I.; Dronyuk, I.; Velmurugan, A.K.; Swapna, B. Novel Hybrid Optimization Techniques to Enhance Reliability from Reverse Osmosis Desalination Process. *Energies* **2023**, *16*, 713. [CrossRef]